

Simulation Assisted Current Density Monitoring for Lithium-ion Batteries in Electric Vehicles

Mehrnaz Javadipour*, Seyed A Alavi, Kamyar Mehran

School of Electronic Engineering and Computer Science, Queen Mary University of London, London, UK

*E-mail: m.javadipour@qmul.ac.uk

Keywords: Battery monitoring, current density, electric vehicles, lithium-ion, simulation assisted modelling.

Abstract

Lithium-Ion batteries (LiBs) are the commonly used energy storage technology in electric vehicles (EVs), plug-in hybrid electric vehicles (PHEVs) and electric bikes (EBs), due to their inexpensive manufacturing cost. In order to use the batteries optimally and to increase their lifetime, reliable state of health (SoH) monitoring solutions are required to be included in the battery management system (BMS). This paper proposes a simulation assisted electrode and electrolyte current density monitoring for lithium-ion batteries that can considerably increase the SoH estimation accuracy. The proposed method is realized through the fusion of the information from the magnetic field sensors, installed on the surface of battery pouch cells, together with the online simulation of the battery dynamic model, in real-time. The simulation data is fed from the measurements of the already installed BMS. The battery model is developed in COMSOL modelling software and the data fusion is implemented on dSPACE Microlabbox real-time simulator. The results confirm that the proposed monitoring solution can be potentially used to provide a highly accurate estimation system for EV battery pouch cells.

1 Introduction

Electric vehicles (EVs) and renewable power sources are the examples of modern technologies, which are developed based on the advances in storing energy [1–3]. EVs require energy storages for their operational longevity and distributed renewable generations (e.g. wind turbines and photovoltaic panels) use energy storages to support energy reserve due to their intermittent characteristic [4–6].

From all the energy storage technologies, Lithium-ion batteries (LIBs) are commonly used due to their inexpensive manufacturing costs and easier maintenance. LIBs, comparing to their older technologies, have longer life cycles, higher rate of charge/discharge, and high energy density, resulting in high capacity storages suitable for industrial use cases [7, 8].

In contrast to their many advantageous, LIBs require a reliable condition monitoring system that is able monitor their state of health (SoH) and state of charge (SoC) due to the safety and operational issues associated with them. There are high chances of fire or explosion when the LIBs are used in high temperature environments or under short circuit faults [9]. Therefore, it is mandatory to include a degree of operational awareness in the battery management systems (BMS).

Condition monitoring of LIBs is usually summarized as SoC and SoH estimation in the literature. Ageing is the main factor for SoH estimation. LIBs have a limited number of charging/discharging cycles that makes them unusable after a while [10]. Large research efforts have been made to understand ageing in Li-ion batteries [11–13]. Along with that, mechanical degradation in LIBs is another factor that affects the SoH in a battery. The monitoring of SoC and SoH in LIBs has been studied in several papers [13–15]. In [14], the measurement of small

induced magnetic field changes in a cell have been studied to be used for assessment of the level of lithium incorporation into the electrode materials and to detect certain defects in a cell. In [13], the role of negative electrode porosity in long-term ageing of LIBs has been analysed. It was shown that the lithium can only participate to SEI (solid electrolyte interphase) growth, which decreases the capacity by lithium consumption.

The commonly used techniques for SoC estimation such as terminal voltage measurement and coulomb counting are not accurate enough to model the ageing in performance degradation in LIBs. This is due to the nature of the LIBs, which internally consist of different complex non-linear chemical processes. Although the manufacturing cost of LIBs is decreasing every year, still, high capacities are expensive and require a suitable monitoring system for longer operation.

Therefore, a low-cost battery monitoring method is required in order to improve the utilization efficiency, to maximize the lifetime and to guarantee the safe operation. To address this issue, this paper proposes a simulation assisted electrode and electrolyte current density monitoring method for lithium-ion batteries that can considerably increase the SoH estimation accuracy.

The proposed method is realized through the fusion of the information from the magnetic field sensors, installed on the surface of battery pouch cells, together with the online simulation of the battery dynamic model, in real-time. The simulation data is fed from the measurements of the already installed BMS. The battery model is developed in COMSOL modelling software and the data fusion is implemented on dSPACE Microlabbox real-time simulator. The results show that the proposed method can be potentially used for providing a highly accurate estimation system for EV battery pouch cells.

2 Magnetic field imaging of batteries for state estimation improvement

For the practical part of the project, the magnetic field images are captured directly by attaching an array of multiple magnetic sensors on the Nissan Leaf cell. In Fig 1 a flow diagram of magnetic field imaging process is illustrated.

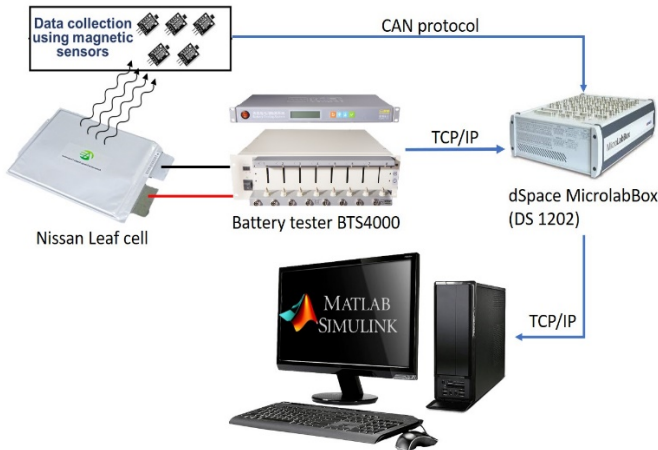


Fig. 1. Flow diagram of magnetic field imaging process.

The eight-channel battery testing (BTS-4000) along with its control unit, is an equipment basically used for testing and controlling purposes.

In this project they are used to generate different charging/discharging load cycles for the cell. The battery tester is connected to the Microlabbox via TCP/IP connection. In order to record the load current and output voltage waveform of the cell, using an interface was mandatory, which here we used the dSPACE Microlabbox (DS-1202).

This equipment was also used for collecting the magnetic data obtained from the magnetic sensors. The recorded data is then processed by Matlab/Simulink estimation model for online parameter estimation of the equivalent circuit model of the battery.

In Fig 2 the actual setup of magnetic field imaging of the cell is showed. The operation of the magnetic sensors we are using in this project is based on the hall effect phenomenon. Each sensor can measure the magnetic field intensity up to ± 2 mT.

Magnetic field images were taken during different conditions under charge cycles of the battery so that there would be a reliable reference available for each state in the cell.

3 Practical and simulation results

Creating an accurate electrochemical model of the cell is necessary for studying the performance of the battery. This method is also used for comparing the expected and the actual results in the case study. In order to validate the achieved experimental results from the Nissan Leaf battery, a complete and accurate electrochemical simulation of the cell is developed using the COMSOL Multi-physics software.



Fig. 2 Placement of the sensors on the surface of the cell for directly measuring the magnetic field for online magnetic field monitoring while charging.

COMSOL considers a vast set of parameters and has a complete library for each element used to manufacture the cell. During the simulation, the value of almost every parameter used in the model was available in the software's libraries. Therefore, it can be concluded that simulation using COMSOL for validating results in this project is a proper method.

The physical parameters of the battery, as well as the materials of the electrodes and the electrolyte inside of the cell, are assigned to the domains of the simulated model. Table 1 shows the physical parameters and dimensions of the simulated cell. The parameters related to the materials used in the cell are derived from [15].

A thorough research has been done to find the most accurate values for particle radius, porosity and maximum host capacity for both positive and negative electrodes, to achieve the possible real results [13, 14].

3.1 Magnetic field images on top of the positive electrode of an old cell during 10A charging

The NMC/Graphite cell model simulated in COMSOL has the same size and parameters comparing to the one we used for practical experiments in the lab. While charging the existing

Table 1 Physical parameters of the Nissan Leaf cell.

Name	Expression	Description
L_sep	30[um]	Separator thickness
L_pos	60[um]	Positive electrode thickness
L_neg	60[um]	Negative electrode thickness
L_pos_cc	10[um]	Positive current collector thickness
L_neg_cc	10[um]	Negative current collector thickness
W_cell	216[mm]	Cell width
H_cell	290[mm]	Cell height
H_tab	1[cm]	Tab height
W_tab	14[cm]	Tab width
L_cell	L_sep+L_pos+L_neg +L_neg_cc/2 +L_pos_cc/2	Cell thickness

old Nissan Leaf cell in the lab with a charging current of 10A, the magnetic sensors were placed on the cell to capture the value of the magnetic field across the current collector of the cell. In Fig 3, MFIs captured in different states of charge of the cell during the 10A charging is illustrated. It is shown that the magnetic field intensity around the positive tab, where the input voltage is applied, is higher than the rest of the cell.

Simulations in COMSOL validated these results. The MFIs generated in different states of charge of the cell during the 10A charging of the simulated model is illustrated in Fig 4.

According to the Maxwell's original circuital law, magnetic field is proportional to current density. Therefore, it is understood that the current density images (CDIs) across the cell will have the same pattern comparing to the MFIs.

As the experimental results are successfully validated by the simulation model in COMSOL, it is proved that the model is close enough to the reality. Therefore, further investigations on the current density distribution inside of the cell can be carried out using the model.

3.2 Proposed methodology to improve current density monitoring

According to the final MFIs in different states of charge, illustrated in Fig 4.2, it was observed that almost the same pattern and numbers for each colour-band repeated as the battery went from fully discharged to fully charged and no noticeable changes happened in the magnetic field captured by the sensors placed on the top of the positive current collector of the cell.

This result seems to be natural as the current collector is made of Aluminium and it somehow acts like a Faraday cage and blocks large amount of electromagnetic wave produced inside of the cell. Therefore, it is concluded that the current methodology to monitor the magnetic field generated by the

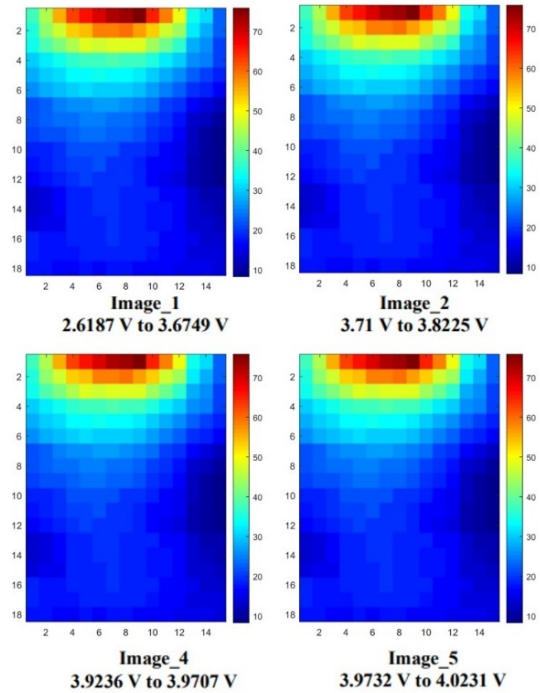


Fig. 3 Lab experiment results: MFIs captured in different states of charge of the cell during the 10A charging – units are in micro Tesla [uT] and tabs are placed on top of the image.

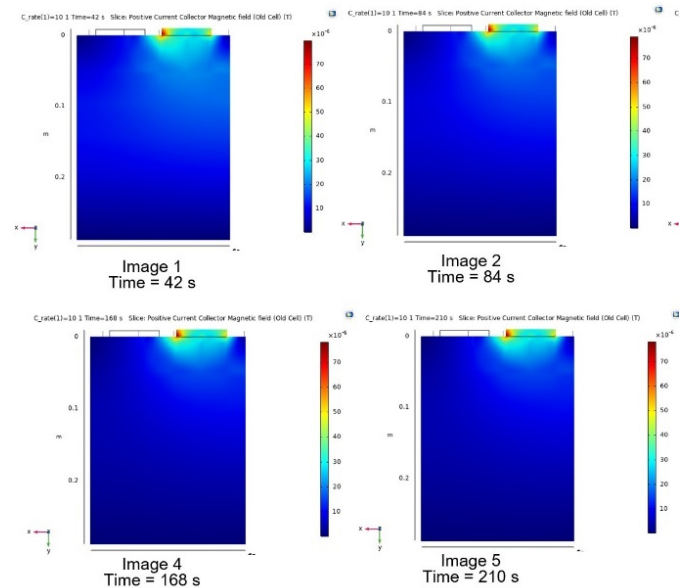


Fig. 4 COMSOL simulation results: MFIs generated in different states of charge of the cell during the 10A charging – units are in micro Tesla [uT] and tabs are placed on top of the image.

battery in its different states of charge has been failed to show a meaningful result.

By studying the simulated model in COMSOL it was understood that the current density distribution and intensity does change in the cell in different states of charge, but this change

is happening in between the current collectors, inside of the both positive and negative electrodes and also in the electrolyte of the cell. Fig 5 shows the simulation results of CDIs change in the positive electrode of the cell, just under the positive current collector, during the 10A charging.

It is observed that the current density distribution pattern changes gradually in the positive electrode. During the charging process, the current density across the cell will be uniform for a short period of time and then, the intensity around the tabs reaches the lowest level compared to the rest of the cell. This pattern of distribution of the current density remains until the cell is nearly charged and only the assigned value to each band changes.

CDIs also changed inside of the electrolyte of the cell during the charging process. Fig 6 shows the simulation results of CDIs change in the middle of the electrolyte of the cell during the 10A charging.

It can be concluded that by monitoring the magnetic field and subsequently, the current density inside of the positive electrode or the electrolyte, it would be possible to find a meaningful relation between the captured images and the SoH of the cell.

Current density distribution inside of the electrolyte follows a similar pattern comparing to the images taken from the positive electrode, therefore, by inserting the magnetic sensors under the Aluminium current collector, it would be possible to record the actual internal behaviour of the cell.

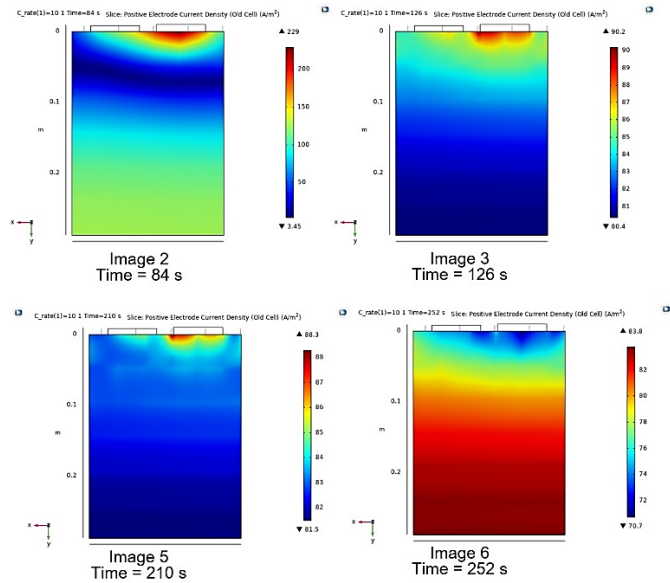


Fig. 5 COMSOL simulation results: CDIs generated in the positive electrode of the cell at different states of charge during the 10A charging

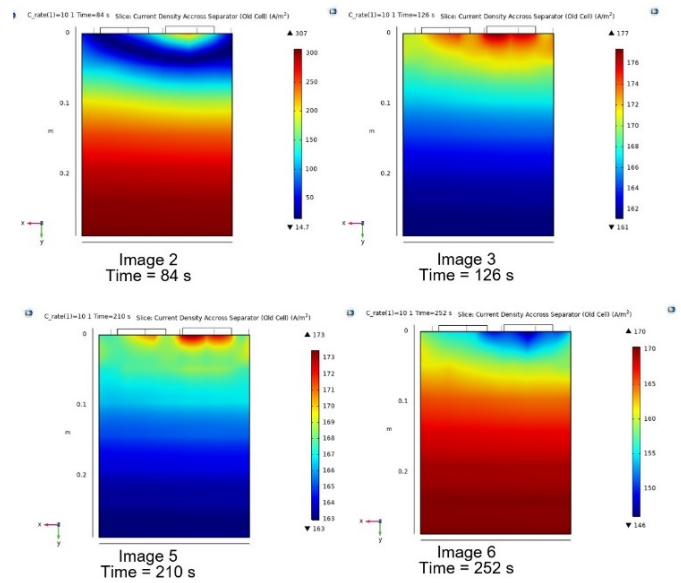


Fig. 6 COMSOL simulation results: CDIs generated in the middle of the electrolyte of the cell at different states of charge during the 10A charging

3.3 CDIs derived from simulated model of the cell, in different circumstances

The most important feature, which indicates the SoH in a battery, is the maximum available capacity of the cell. The capacity of the simulated cell depends on the physical and chemical parameters of the battery, as well as on the maximum and minimum SoC difference in the cell. The SoC is a parameter with no units and it is usually defined in percent. The simulated battery is studied during the constant current 5-A charge situation under the three different conditions:

1. for a brand-new or a fresh cell: with a maximum full-charge capacity of %97.5
2. for a relatively aged cell: with a maximum full-charge capacity of %85
3. for an old cell: with a maximum full-charge capacity of %60

It was observed that the current density reached a maximum peak in the middle of the charging mechanism and on that point, the difference between the maximum and the minimum level of the current density became the greatest. Fig 7, Fig 8, and Fig 9 specially shows the peak of the current density across the positive electrode in the cell.

It is observed that there is a negligible difference between the two CDIs shown in Fig 8 and Fig 9, as the minimum value of current density distributed at the endpoints of the fresh cell, is slightly greater than in an aged cell and obviously, it is much greater than in an old cell. These images then can be used in machine learning processes for future studies. Moreover, as it is shown on the colour bands, the difference between the maximum and minimum level of current density in a fresh cell, a relatively aged cell and an old cell are 621.12

C_rate(1)=5 1 Time=80 s Slice: Positive Electrode Current Density (Fresh Cell) (A/m²)

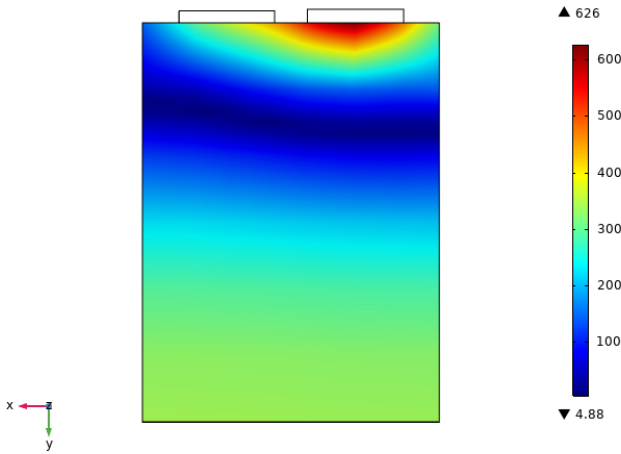


Fig. 7 CDI generated in the simulated model of a fresh cell in the middle of 5A charging

C_rate(1)=5 1 Time=80 s Slice: Positive Electrode Current Density (Old Cell) (A/m²)

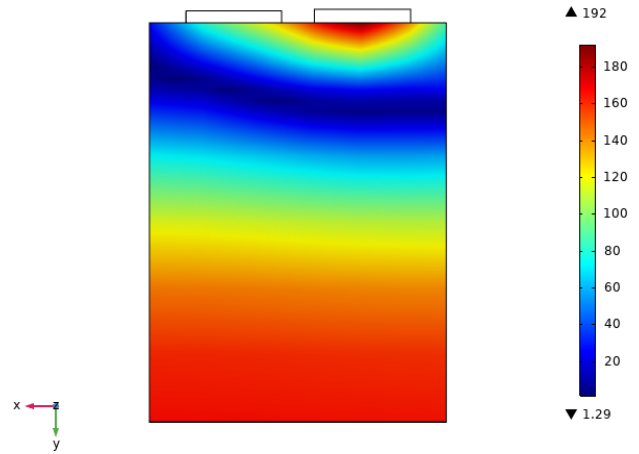


Fig. 9 CDI generated in the simulated model of an old cell in the middle of 5A charging

C_rate(1)=5 1 Time=80 s Slice: Positive Electrode Current Density (Aged Cell) (A/m²)

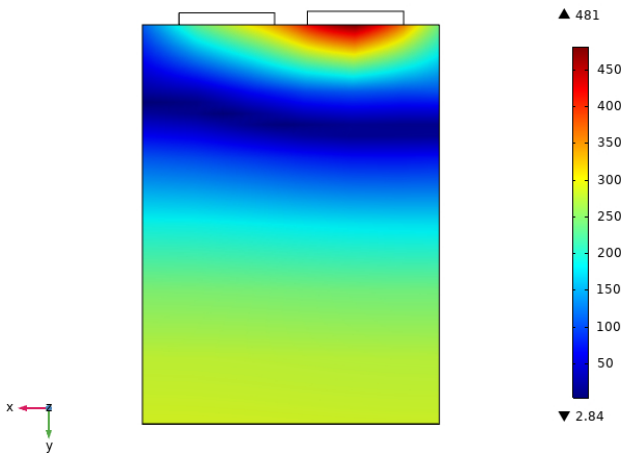


Fig. 8 CDI generated in the simulated model of a relatively aged cell in the middle of 5A charging

[A/m²], 478.16[A/m²] and 190.71 [A/m²], respectively. It can be concluded that as a cell ages, the magnetic field intensity or the current density distribution across the cell becomes more uniform.

4 Conclusion

Early achieved results show that the new proposed method of online current density monitoring in lithium-ion batteries has the potential to improve the state estimation system in a cell. By comparing the practical results and simulation results created in COMSOL Multiphysics software, it is validated that the simulated electrochemical model of the lithium-ion cell can be successfully used for further simulation assisted magnetic field and current density monitoring studies. In future, information derived from CDIs would be used for predicting the state of certain parameters of the cell.

- [1] S. A. Alavi, K. Mehran, Y. Hao, A. Rahimian, H. Mirsaedi, and V. Vahidinasab, "A distributed event-triggered control strategy for dc microgrids based on publish-subscribe model over industrial wireless sensor networks," *IEEE Transactions on Smart Grid*, vol. 10, no. 4, pp. 4323–4337, 2019.
- [2] S. A. Alavi, M. Javadipour, and K. Mehran, "Microgrid Optimal State Estimation Over IoT Wireless Sensor Networks With Event-Based Measurements," in *IECON 2019 - 45th Annual Conference of the IEEE Industrial Electronics Society*. IEEE, oct 2019, pp. 4145–4150.
- [3] J. P. Rivera-Barrera, N. Muñoz-Galeano, and H. O. Sarmiento-Maldonado, "Soc estimation for lithium-ion batteries: Review and future challenges," *Electronics (Switzerland)*, vol. 6, no. 4, 2017.
- [4] M. Montazeri, A. Alavi, H. Rahmat Jou, J. Mehr Ardestani, and H. Jadali Pour, "Real time substation distributed control system simulator development based on IEC 61850 standard for a sample substation: Case study: Sheikh bahayi substation 400/230/63KV," in *Smart Grid Conference 2013, SGC 2013*. IEEE, dec 2013, pp. 108–112.
- [5] S. Amir Alavi, A. Rahimian, K. Mehran, and J. Alaleddin Mehr Ardestani, "An IoT-Based Data Collection Platform for Situational Awareness-Centric Microgrids," in *Canadian Conference on Electrical and Computer Engineering*, vol. 2018-May. IEEE, 2018, pp. 1–4.
- [6] Z. B. Omariba, L. Zhang, and D. Sun, "Review on health management system for lithium-ion batteries of electric vehicles," *Electronics (Switzerland)*, vol. 7, no. 5, 2018.
- [7] A. Alavi, M. Javadipour, and A. A. Afzalian, "An optimal event-triggered tracking control for battery-based wireless sensor networks," in *2016 Smart Grids Conference, SGC 2016*. IEEE, dec 2017, pp. 42–47.
- [8] H. Popp, M. Koller, S. Keller, G. Glanz, R. Klambauer, and A. Bergmann, "State Estimation Approach of

- Lithium-Ion Batteries by Simplified Ultrasonic Time-of-Flight Measurement,” *IEEE Access*, vol. 7, pp. 170 992–171 000, 2019.
- [9] V. Pop, H. J. Bergveld, D. Danilov, P. P. L. Regtien, and P. H. L. Notten, *Battery Management Systems*, ser. Philips Research Book Series. Dordrecht: Springer Netherlands, 2008, vol. 9.
- [10] T. G. Zavalis, M. Klett, M. H. Kjell, M. Behm, R. W. Lindström, and G. Lindbergh, “Aging in lithium-ion batteries: Model and experimental investigation of harvested LiFePO₄ and mesocarbon microbead graphite electrodes,” *Electrochimica Acta*, vol. 110, pp. 335–348, 2013.
- [11] Y. Gao, J. Jiang, C. Zhang, W. Zhang, Z. Ma, and Y. Jiang, “Lithium-ion battery aging mechanisms and life model under different charging stresses,” *Journal of Power Sources*, vol. 356, pp. 103–114, 2017.
- [12] E. Prada, D. Di Domenico, Y. Creff, J. Bernard, V. Sauvant-Moynot, and F. Huet, “A Simplified Electrochemical and Thermal Aging Model of LiFePO₄-Graphite Li-ion Batteries: Power and Capacity Fade Simulations,” *Journal of The Electrochemical Society*, vol. 160, no. 4, pp. A616–A628, feb 2013.
- [13] P. Bernard, H. Martinez, C. Tessier, E. Garitte, S. Franger, and R. Dedryvere, “Role of Negative Electrode Porosity in Long-Term Aging of NMC//Graphite Li-Ion Batteries,” *Journal of The Electrochemical Society*, vol. 162, no. 13, pp. A7096–A7103, 2015.
- [14] P. C. Tsai, B. Wen, M. Wolfman, M. J. Choe, M. S. Pan, L. Su, K. Thornton, J. Cabana, and Y. M. Chiang, “Single-particle measurements of electrochemical kinetics in NMC and NCA cathodes for Li-ion batteries,” *Energy and Environmental Science*, vol. 11, no. 4, pp. 860–871, 2018.
- [15] P. Singh, N. Khare, and P. K. Chaturvedi, “COMSOL Multiphysics® Modelling for Li-ion Battery Ageing,” in *Excerpt from the Proceedings of the 2014 COMSOL Conference in Bangalore*, no. 2013, 2014, p. 2.